doi:10.1016/j.jmb.2005.02.053 J. Mol. Biol. (2005) 348, 445–457

JMB

Available online at www.sciencedirect.com

SCIENCE DIRECT®

ELSEVIER

Architecture of the Ribosome–Channel Complex Derived from Native Membranes

Jean-François Ménétret[1]†, Ramanujan S. Hegde[2]†, Sven U. Heinrich[4] Preethi Chandramouli[1], Steven J. Ludtke[3], Tom A. Rapoport[4] and Christopher W. Akey[1]*

[1]*Department of Physiology and Biophysics, Boston University School of Medicine, 700 Albany St., Boston, MA 02118-2526 USA*

[2]*Cell Biology and Metabolism Branch, National Institute of Child Health and Human Development, National Institutes of Health, 18 Library Drive, Bethesda, MD 20892 USA*

[3]*National Center for Macromolecular Imaging Verna and Marrs McLean Department of Biochemistry and Molecular Biology, Baylor College of Medicine, 1 Baylor Plaza, Houston, TX, 77030 USA*

[4]*Howard Hughes Medical Institute and Department of Cell Biology, Harvard Medical School, 240 Longwood Avenue Boston, MA 02115, USA*

**Corresponding author*

The mammalian Sec61 complex forms a protein translocation channel whose function depends upon its interaction with the ribosome and with membrane proteins of the endoplasmic reticulum (ER). To study these interactions, we determined structures of "native" ribosome–channel complexes derived from ER membranes. We find that the ribosome is linked to the channel by seven connections, but the junction may still provide a path for domains of nascent membrane proteins to move into the cytoplasm. In addition, the native channel is significantly larger than a channel formed by the Sec61 complex, due to the presence of a second membrane protein. We identified this component as TRAP, the translocon-associated protein complex. TRAP interacts with Sec61 through its transmembrane domain and has a prominent lumenal domain. The presence of TRAP in the native channel indicates that it may play a general role in translocation. Crystal structures of two Sec61 homologues were used to model the channel. This analysis indicates that there are four Sec61 complexes and two TRAP molecules in each native channel. Thus, we suggest that a single Sec61 complex may form a conduit for translocating polypeptides, while three copies of Sec61 play a structural role or recruit accessory factors such as TRAP.

Keywords: ribosome–channel complex; Sec61; TRAP; co-translational translocation

Introduction

In all cells, secretory and membrane proteins must be translocated across or integrated into endoplasmic reticulum (ER) membranes, with the help of a protein-conducting channel. The central component of the conserved channel is a heterotrimer of three membrane proteins, termed the SecY complex in bacteria and archaebacteria, and the Sec61 complex in eukaryotes. The largest subunit of this heterotrimer (termed SecY or Sec61α) is a multi-spanning membrane protein that forms the pore of the channel.[1,2] Evidence from prokaryotes and eukaryotes suggests that three to four copies of either the SecY or Sec61 complex may associate to form channels.[3–8] These data have been interpreted to indicate that a translocation pore is formed at the confluence of multiple subunits. However, a recent crystal structure of the archael

† J.-F.M. and R.S.H. contributed equally to this work.

Abbreviations used: ER, endoplasmic reticulum; TM, transmembrane; SPC, signal peptidase complex; OST, oligosacharryl transferase; TRAM, translocating chain associated membrane protein; TRAP, translocon-associated protein complex; RCCs, ribosome–channel complexes; EM, electron microscopy; ES, expansion segments.

E-mail address of the corresponding author: cakey@bu.edu

0022-2836/$ - see front matter

SecY complex suggests that the pore may reside within a single heterotrimer.[9] In 2D membrane crystals, SecY complexes form a dimer with their essential SecE subunits facing each other.[10] This SecY/Sec61 dimer is thought to form the building block of prokaryotic and eukaryotic protein translocation channels.[5,9,11,12]

SecY and Sec61 complexes must associate with partners that provide a driving force for polypeptide transport. In bacteria, post-translational translocation requires a cytosolic ATPase, termed SecA, while in eukaryotes the partners are a tetrameric Sec62/63 membrane protein complex and BiP, an ATPase located in the lumen of the endoplasmic reticulum.[13] Co-translational translocation in all organisms requires the ribosome as the major channel partner. In this pathway, nascent chains exit from a tunnel in the large ribosomal subunit and are transferred into the translocation channel. Co-translational translocation is also responsible for the integration of most membrane proteins. In this process, transmembrane (TM) segments move into the lipid phase through a lateral gate in the channel.[14] In addition, a cytosolic domain that follows a TM segment must exit through the ribosome–channel junction and fold in the cytoplasm. Importantly, the membrane barrier for small molecules should be maintained during all steps of translocation.

The eukaryotic channel associates with additional membrane proteins during co-translational translocation. These include the signal peptidase complex (SPC), the oligosacharryl transferase (OST), the translocating chain associated membrane protein (TRAM) and the translocon-associated protein complex (TRAP). The SPC catalyzes signal sequence cleavage,[14] while the nine subunit OST complex (290 kDa) is responsible for the Asn-linked glycosylation of nascent chains.[15] TRAM is an abundant membrane protein that has been shown to enhance the translocation of some secretory proteins and is located in close proximity to nascent chains.[16–19] The TRAP complex is comprised of four membrane protein subunits. The α, β, and δ-subunits are single-spanning proteins with prominent lumenal domains, while the γ-subunit crosses the membrane four times.[20] TRAP enhances the translocation of nascent proteins that have prolonged access to the cytoplasm[21] and can be crosslinked to nascent chains.[17,22–24] Sequence-based analysis has identified TRAP-related proteins in higher eukaryotes but not in budding yeast. Currently, little is known about the way in which SPC, OST, TRAM and TRAP associate with the Sec61 channel.

Previous studies of ribosome–channel complexes (RCCs) by electron microscopy (EM) provided evidence that Sec61 channels isolated from ER membranes associate with additional membrane proteins. These native channels are noticeably larger than channels containing Sec61 alone, have an elliptical rather than cylindrical cross-section in the plane of the membrane, and contain a prominent lumenal domain.[6,8] Biochemical analyses demonstrated that "native" RCC preparations used for these structures contain several membrane proteins in addition to the Sec61 complex, but only TRAP and OST are abundant enough to contribute to the maps.[6]

We now provide an improved picture of the RCC and identify TRAP within the native channel. TRAP has a tripartite architecture and its prominent lumenal domain is connected to the channel by two stalk-like features. We then modeled the general arrangement of the Sec61 and TRAP complexes in the native channel. Based on this analysis, the native channel in our maps is comprised of four Sec61 and two TRAP complexes. Thus, OST may be disordered in this specimen. Since TRAP is present in nearly all copies of the RCC, this component may play a general role in protein translocation within higher eukaryotes. The pattern of connections between the ribosome and channel suggests that several Sec61 complexes may play a structural role, while at the same time creating docking sites for accessory factors such as TRAP. Thus, only one Sec61 may provide an active pore for protein translocation, as suggested by a recent crystal structure of an archaebacterial SecY complex.[9]

Results

Maps of the native ribosome–channel complex

To generate native RCCs in a defined state, we used a procedure developed previously.[8] In this approach, translating ribosomes were removed from rough microsomes with puromycin and high salt. These stripped ER membranes were then incubated with ribosomes which contained a tRNA in the exit-site,[8] and floated in a sucrose gradient. The RCCs were then solubilized from the membranes in deoxy-BigCHAP (DBC) containing buffer, isolated by centrifugation, and flash frozen on a carbon-coated grid in buffer. These native RCCs contain the Sec61 complex, TRAP, and OST in amounts comparable to ribosomes, while other membrane proteins are present in much lower amounts and thus, do not contribute to the maps. To obtain better resolution, we collected a large number of particles (~154,000) and processed them in EMAN.[25] A final map with a resolution of 10 Å ($FSC_{0.5}$) was calculated from ~104,000 particles (Table 1, Figure 1(a)). Surface views of the RCC from this map are shown in Figures 1(c) (front) and 2(b) (bottom). This is the first reported structure of a mammalian ribosome with a resolution of ~10 Å. Since the protein translocation channel is the focus of this report, a detailed analysis of the ribosome will be published elsewhere (J.M. *et al.*, unpublished results). However, a number of features deserve comment. First, a tRNA is present in the exit-site between the small and large ribosomal subunit; hence, ribosomes in this specimen are in a defined state (Figure 1(c)).[8] Second, there are six large

Table 1. 3D analyses of ribosome–channel complexes

RCCs	Micrographs	Magnification	Å/pixel	Number of particles selected and in the final maps	Resolution (Å) (FSC $_{0.5}$)
Native RCC	423	50,000×	2.73	154,000/104,000	10
RCC with poly-lysine	192	50,000×	2.73	84,000/29,000	14.7
Trap-depleted	37	29,000×	3.14	21,000/17,000	26
Trap add-back	35	29,000×	3.14	36,500/17,000	26
Totals:	687			295,500/167,000	

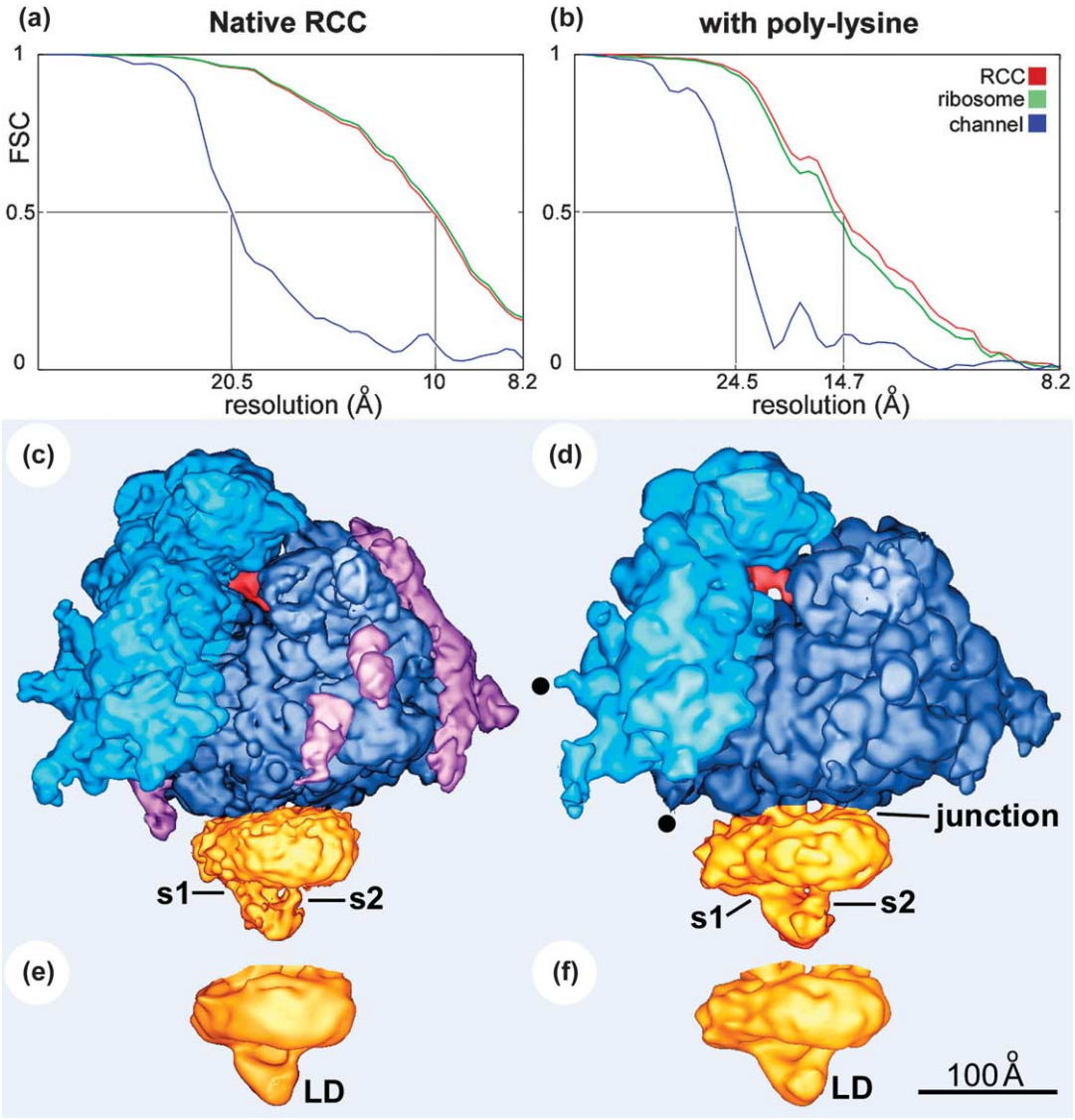

Figure 1. The native ribosome–channel complex. (a) A Fourier shell curve is shown for the native RCC prepared on carbon film, which has a resolution of 10 Å (red line), while the channel has a resolution of ∼20 Å (blue line). (b) A Fourier shell curve is shown for the native RCC made with poly-lysine coated, carbon films. The ribosome has a resolution of 14.7 Å while the channel has a resolution of ∼24 Å. (c) A frontal view of the native RCC is shown, low pass filtered at 10 Å resolution. Small and large subunits are colored in light blue and dark blue respectively. The channel is colored gold, the expansion segments are purple and the E-site tRNA is red. Primary (s1) and secondary (s2) stalks on TRAP are indicated. (d) A frontal view is shown of the RCC map prepared with poly-lysine coated grids and is filtered to 14.7 Å resolution. The primary and secondary stalks of TRAP are indicated (s1, s2) and the junction is labeled. Some exposed RNA helices are markedly reduced in size (indicated with black dots), due to interactions with poly-lysine. (e) A side view of the native channel is shown after low pass filtering to 20 Å resolution. The TRAP lumenal domain (LD) is marked. (f) A side view of the native channel prepared with poly-lysine is shown at ∼24 Å resolution.

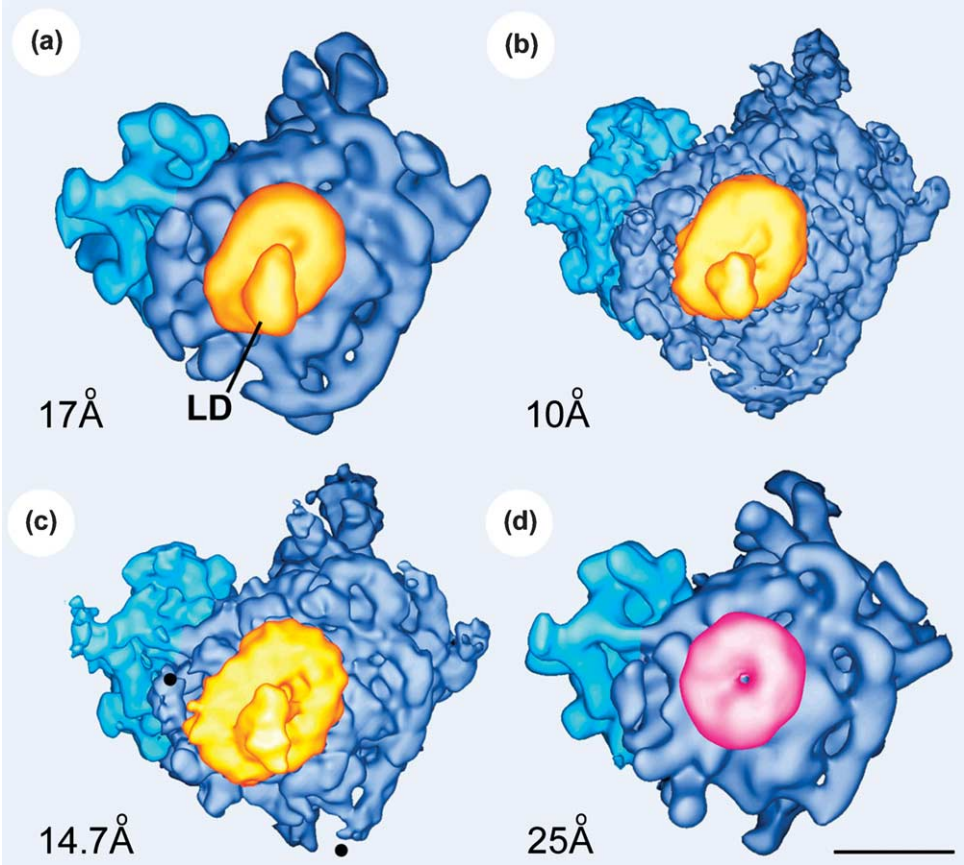

Figure 2. A comparison of ribosome–channel complexes. (a) A bottom view is shown of a published, native RCC map at 17 Å resolution.[8] The lumenal domain (LD) is indicated. (b) A bottom view is shown of the native RCC map at 10 Å resolution, with the channel filtered to 20 Å resolution. (c) A bottom view is shown of the native RCC map made with poly-lysine coated grids and filtered at 14.7 Å resolution. The channel is much larger than in previous maps and has been filtered to 20 Å resolution, to allow a better comparison with Figure 1(a) and (b). Black dots mark regions of exposed rRNA that have been disordered by interactions with poly-lysine (compare with (b)). (d) A bottom view is shown of a published RCC map made with rabbit ribosomes, purified canine Sec61 and a nascent chain.[6] The map is at a resolution of ~25 Å and the scale bar represents 100 Å.

expansion segments (ES) in the 28 S rRNA that form spines on the surface of the large subunit (highlighted in purple, Figure 1(c)).[26–28,8] Third, there are new features present, which include additional connections between the ribosome and channel (see next section), and a second stalk between the lumenal domain and the channel (s2 in Figure 1(c)).

Unfortunately, this map does not show high resolution details of the Sec61 subunits, perhaps because the channel is somewhat flexible. To evaluate this possibility, we used QSegment in EMAN,[25] and 3D maps from half datasets, to create volumes that contained either the ribosome or the channel. Separate resolution curves for the ribosome and the channel were then calculated from the appropriate volumes. Using this approach, we found that the resolution of the ribosome is similar to the whole RCC, while the channel lags behind with a resolution of ~20 Å (Figure 1(a)). Therefore, we filtered the channel to a resolution of 20 Å (Figures 1(e) and 2(b)). We also analyzed the angular distribution of the particles and found that RCCs have a preference for binding to the EM grid with their channels in contact with the carbon support film (not shown). Thus, we reasoned that the channel may be distorted by interactions with the carbon support film. An alternate approach would be to freeze RCCs over holes; however, this has not been possible due to their low concentration and tendency to aggregate.

We devised an alternate preparative method in which carbon grids treated with poly-lysine were used to bind RCCs through exposed, negatively charged regions (cf. rRNA). We collected ~84,000 particles from this specimen and calculated a 3D map from the best complexes (Table 1; Figures 1(d) and 2(c)). The resolution of this map is ~14.7 Å ($FSC_{0.5}$, Figure 1(b)) and some surface-exposed rRNA features are lost due to interactions with poly-lysine (marked with black dots in Figures 1(d) and 2(c)). The angular distribution of particles in this dataset is nearly random. Thus, the channel does not contact the carbon support film in many of the particles. This geometry may account for the marked increase in the overall size of the channel in this map, when compared to previous structures

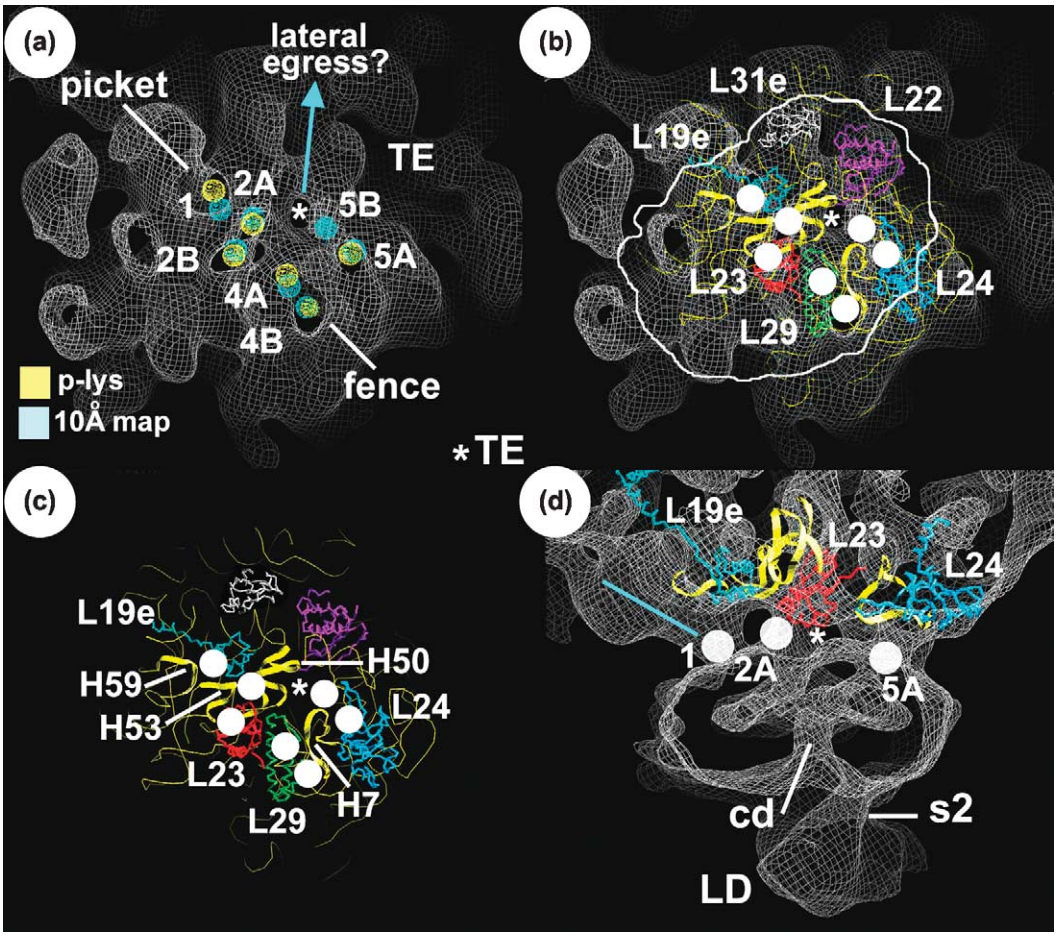

Figure 3. Connections between the channel and the large ribosomal subunit. (a) A thin slab of density from the RCC map made with poly-lysine coated grids is shown in the graphics program "O".[46] This slab is centered on the junction between the channel and large subunit. Connections are indicated by cyan circles (from the 10 Å map) and gold circles (from RCCs adsorbed to poly-lysine grids) and are labeled. The C2 and C4 connections are bifurcated into 2A/2B and 4A/4B when the entire map is viewed. New connections (5A and 5B) were found near the tunnel exit (TE). The excellent correspondence of the connections in the two maps suggests that their positions are reliable. A possible path for the nascent chain into the cytoplasm is indicated by a blue arrow. (b) The atomic structure of the channel docking surface from the *Haloarcula* large subunit is shown, with relevant proteins labeled and important rRNA regions highlighted as yellow ribbons. Connections are marked with white dots and the tunnel exit is indicated on the meshwork from the RCC map made with poly-lysine coated grids. The outline of the native channel is also shown. (c) A bottom view of the large subunit is shown with the wire mesh from the 3D map removed. Regions of the large subunit that may help form the connections are labeled (see the text). (d) The ribosome–channel junction is shown from the front of the channel, as viewed along the plane of the ER membrane. Connections 1, 2A and 5A are marked, along with the ribosomal proteins and rRNA segments that may contribute to their formation. Note that connection 1 involves a novel feature in the eukaryotic ribosome (marked with a blue line), in addition to possible contributions from L19e (RL19) and h59. The lumenal domain of TRAP (LD) and the secondary stalk (s2) are indicated, along with the central depression (cd).

(Figure 2(a)–(c)). In addition, the native channel is significantly larger than one comprised of purified Sec61 (Figure 2(d)).[6] However, an FSC curve calculated from this native channel gives a resolution of ~24 Å (Figure 1(b) and (f)), which still lags behind the ribosome. We surmise that connections between the channel and the ribosome may be flexible enough to preclude us from obtaining a higher resolution map of the channel, when the alignment is driven by the ribosome. Of course, this effect may be exacerbated by interactions between the channel and the support film. Nevertheless, the channels in the new 3D maps are of better quality than those in previous maps, due to the extensive averaging. The maps also provide a basis for analyzing interactions between the channel and the ribosome, as this region is much better defined than previously. In addition, the resolution of the ribosome itself is much higher, which improves the accuracy of our analysis of the connections.

Connections in the ribosome–channel junction

We used the new maps to re-evaluate the junction between the ribosome and the channel. In particular, the junction has a more solid appearance in surface views when compared to previous structures (Figure 1(c) and (d); see the work done by

Ménétret *et al.*[6], Beckmann *et al.*[7] and Morgan *et al.*[8]). In total, there are seven connections between the channel and the large subunit in the map determined at 10 Å resolution (Figure 3(a), cyan circles). These connections overlay well with six connections observed in RCCs adsorbed with polylysine to the carbon film (Figure 3(a), gold circles); hence, these features are reliable. In previous studies, connections 2 and 4 were each considered to be single links,[7,8] but they are now bifurcated (labeled 2A/2B and 4A/4B). Together with connection 1, they form a picket fence across the cytoplasmic surface of the channel that dominates the junction (Figure 3(a)). In addition, a new connection (C5) is visible, due to the higher signal-to-noise ratio in these maps. Connection 5 is located adjacent to the tunnel exit and is bifurcated in the 10 Å map (Figures 3(a) and 5(a) and (b)).

To identify ribosomal components that may contribute to the connections, we manually docked high resolution structures of the eubacterial small[29] and archael large subunits[30] into our maps. The overall fit of the atomic models in the 10 Å map of the canine ribosome is excellent, as shown in serial sections of the large subunit in Image 1 (Supplementary Material). This fitting was guided by many features of the ribosome, including alignment of the exit tunnel. In addition, the channel docking surface on the large subunit is highly conserved, although there are additional loops present in many of the ribosomal proteins.[8] Based on this fit, we evaluated ribosomal proteins and regions of 28 S rRNA that may contribute to the connections (Figure 3(b)–(d)). Connection 1 is formed in part by protein L19e (RL19 in mammals) and helix 59 (Figure 3(b)–(d)). The C1 connection appears to be unique, in that it also involves a region of the eukaryotic ribosome

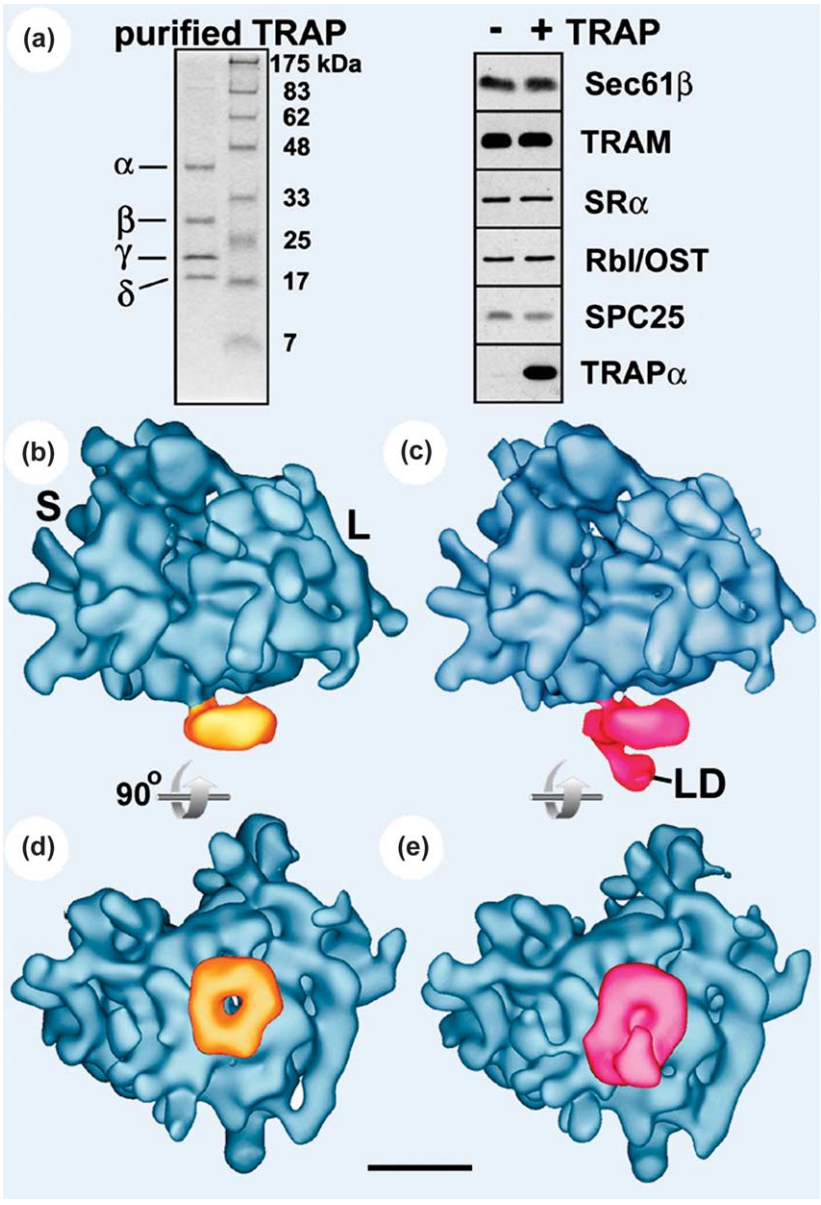

Figure 4. Structure of the RCC without and with TRAP. (a) (left) An SDS polyacrylamide gel of purified TRAP is shown. (right) Reconstituted ER vesicles were prepared without (left) and with TRAP (right), run on SDS PAGE and blotted with antibodies against the indicated proteins (see the text). (b) A frontal view is shown of a map from RCCs made without TRAP. The small subunit (S) is on the left and the large subunit (L) is on the right. The Sec61 channel is colored in gold. (c) A frontal view is shown of a map from RCCs with TRAP added back. The larger channel with a lumenal domain is colored red. (d) A bottom view is shown of the RCC without TRAP. (e) A bottom view is shown of the RCC with TRAP added back. The finger-like lumenal domain points directly towards a dimple that likely represents a central depression between Sec61 subunits. The scale bar represents 100 Å.

that is not present in prokaryotes (blue line in Figure 3(d)). The C2A and C2B connections appear to be formed in part by L23 (RL2B). In addition, C2A may have contributions from helices 53 and 50 in the 28 S rRNA, while C2B may contact the 3′ end of helix 53 (nt 1506–1511). In a previous map, connection C3 was observed as a weak grazing interaction between helix 24 and the channel.[8] However, it is only seen at lower thresholds in these maps (not shown) and thus, may be less significant than the other connections. The C4A and C4B connections may each contact L29 (RL35) and helix 7 (Figure 3(b) and (c)). Finally, connection 5A appears to be formed by L24 (RL26; Figure 3(b)–(d)), while C5B may contact both L24 and helix 7.

In summary, our analysis reveals a ribosome–channel junction that contains more connections than previously thought. In particular, five connections (C1, C2A, C2B, C4A and C4B) form a picket fence that crosses the top of the channel and additional connections are located next to the tunnel exit (C5A/C5B). Nevertheless, there is still ample space between the ribosome and the channel to allow cytoplasmic domains of nascent membrane proteins to move into the cytosol, when they emerge from the ribosomal exit tunnel. Indeed, one possible route involves passage of the nascent chain between connections 2A and 5A/5B (blue arrow in Figure 3(a)).

Identification of TRAP in native channels

Our maps of the native channel contain at least one additional, ordered component that may correspond to either the TRAP or OST complexes.[6,8] To ascertain whether the additional component is TRAP, we combined selective depletion and reconstitution approaches with electron cryo-microscopy of RCCs. Ribosome-depleted ER membranes were solubilized in DBC buffer and the extract was passed over an anion exchange column to remove TRAP, as other translocation components do not bind to this column.[16,21] Proteoliposomes were then reconstituted from this TRAP-depleted extract. In parallel experiments, TRAP was purified (see SDS PAGE gel in Figure 4(a), left panel) and added back to the depleted extract at a concentration equivalent to its original level, prior to membrane reconstitution. The two sets of proteoliposomes were essentially identical except for their TRAP content, as shown by blots against Sec61β, TRAM, the SRP receptor alpha subunit (SRα), ribophorin I (an OST subunit), SPC25 and TRAPα (Figure 4(a), right panel). Both sets of proteoliposomes were equally efficient in the translocation of preprolactin, a substrate that does not require TRAP function (not shown). In addition, the TRAP add-back proteoliposomes stimulated prion protein translocation, which indicates that purified TRAP is active.[21] To generate specimens for EM, non-translating ribosomes were added to the proteoliposomes, the membranes were floated, solubilized and the RCCs were pelleted.

To obtain 3D maps from TRAP-depleted and TRAP add-back specimens, we used *multirefine* in EMAN to sort particles into groups with and without channels (Table 1). Due to the complexity of these experiments, which involved fractionated extracts and reconstituted proteoliposomes, the maps were not of the same quality as those made with native membranes. Nevertheless, both front (Figure 4(b)) and bottom views (Figure 4(d)) demonstrated that the TRAP-depleted channel is similar in size to that seen with purified Sec61 (Figure 2(d)).[6] On the other hand, the channel with re-added TRAP is similar to that observed in the native RCC, because it is elliptical in shape and shows the characteristic lumenal domain (Figure 4(c) and (e)).[6,8] Since the depleted and add-back samples were prepared and analyzed in parallel, we overlayed the maps to reveal the contribution of TRAP to the native channel (Figure 5(a) and (b)).

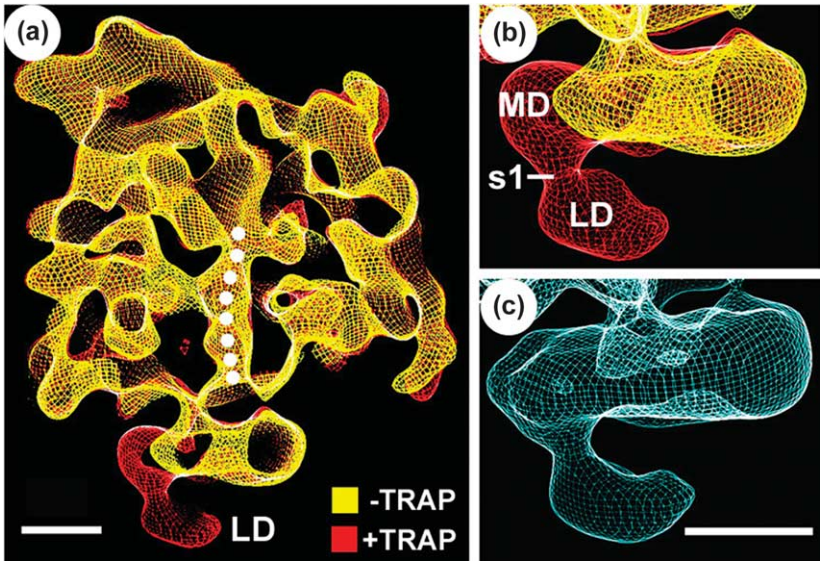

Figure 5. TRAP has a tripartite architecture. (a) Maps of the RCC with (red) and without TRAP (gold) are overlayed in "O".[46] The exit tunnel is marked by white dots and the scale bar represents 50 Å. (b) A close-up of the channel highlights the tripartite architecture of TRAP, which is comprised of a membrane domain (MD), a primary stalk (s1) and the lumenal domain (LD). (c) For comparison, the native channel from a published 17 Å map of the RCC is shown in a similar orientation.[8] The scale bar represents 50 Å.

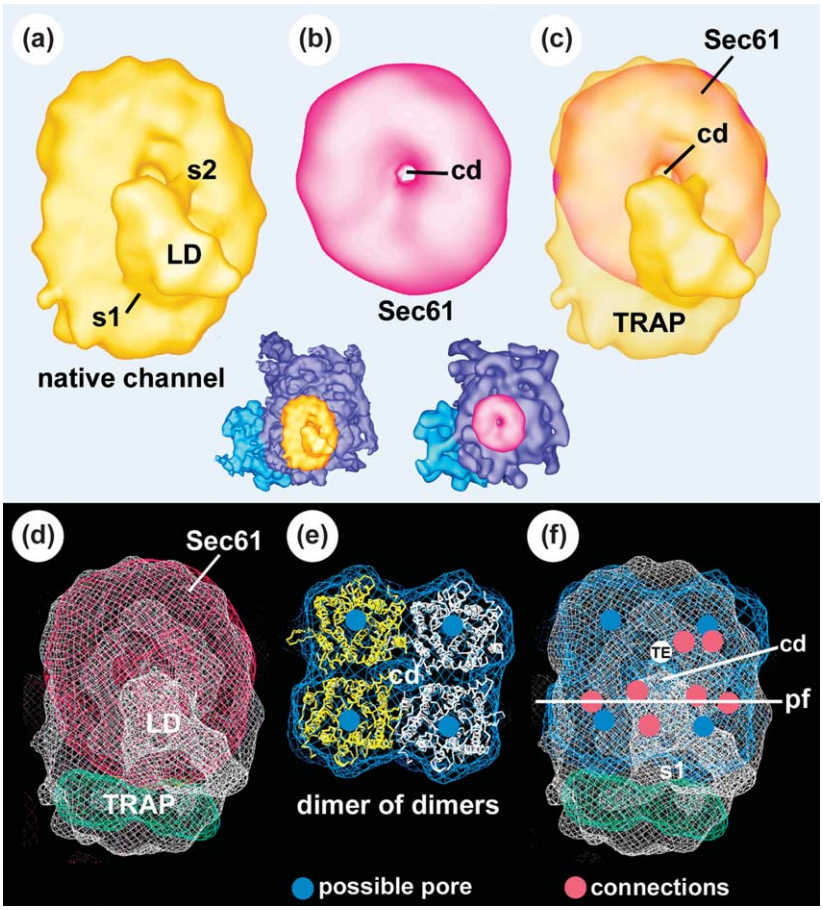

Figure 6. Modeling the native channel. (a) The native channel is viewed from the ER lumen as a solid surface. The lumenal domain (LD) and stalks (s1 and s2) are labeled. (b) After aligning their respective ribosomes, the purified Sec61 channel is shown in red. The central depression is marked with a "cd". Insets show the respective RCCs in the same orientation as (a) and (b). (c) The purified channel is shown overlayed with the native channel. Based on our data, TRAP is located at the back of the channel and is comprised of a membrane domain, a major stalk and a lumenal domain with a second stalk-like connection to the channel. (d) The purified channel (in red mesh) is shown within the white mesh of the native channel in "O", with two bacteriorhodopsin molecules (in green mesh) docked into the back of the channel, to demonstrate that there is room for 14 TMs in this region. This view is from the ER lumen. (e) Two SecY dimers (gold and white ribbons) were docked into the map determined from 2D crystals of SecY[10] to create a dimer of dimers. This packing arrangement creates a central depression (cd). The cryptic pores of the four possible subunits are indicated with blue dots. (f) For one possible model, the molecular envelope from a pair of SecY dimers is shown docked into the native channel in "O" (as viewed from the ER lumen). The relative positions of the four putative pores (blue dots), the tunnel exit (white dot) and the connections (red dots) are shown. The picket fence (pf) formed by five connections is indicated by a white line. Note that two of the possible translocation pores are located behind the picket fence, at the back of the channel. Thus, a nascent chain emerging from the exit tunnel would probably not have access to them. A similar arrangement of the pores occurs when the model is rotated 90 degrees (not shown).

Based on this analysis, TRAP consists of a membrane domain attached *via* a primary stalk to a prominent lumenal domain. Moreover, the membrane domain of TRAP forms a lateral extension that accounts, in part, for the elliptical shape of the native channel. Since OST was present in these specimens, the data suggest that OST may be disordered by the isolation protocol or by interactions with the carbon support film.

In other experiments, we found that the Sec61 complex remained bound to ribosomes, whether or not TRAP was present, and OST sediments with ribosomes and Sec61 in the absence of TRAP (not shown). This suggests that OST and TRAP may interact separately with the channel. In addition, technical problems with these membrane proteins precluded some experiments from being done. For example, RCCs made with purified Sec61 and TRAP were badly aggregated, while our approach of isolating these complexes directly from ER membranes minimizes this problem.

Modeling TRAP in the native channel

TRAP accounts for ~25% of the total membrane area in the native channel and its abundance in mammalian ER is similar to Sec61, which is present in three to four copies per channel.[7,8,31] This suggests that multiple copies of TRAP may be present in the channel, in agreement with cross-linking data, which showed that two TRAP α-subunits are close to each other.[23] To test this possibility, we chose our best map from RCCs made with purified Sec61 and a nascent chain[6] (Figure 2(d)), in which a P-site tRNA was clearly present. This map was docked into the structure of the native RCC using the ribosome for alignment, to avoid bias in positioning the channels. This docking shows that Sec61 forms the entire front of the native channel (Figure 6(a)–(c)) and indicates that there is adequate room at the back of the channel for two TRAP molecules, detergent and lipid. This was demonstrated by modeling TRAP with a bacteriorhodopsin molecule, which has seven TMs as predicted

for TRAP. We find that two bacteriorhodopsin monomers can be placed at the back of the channel (Figure 6(d), in green). Thus, our structures and crosslinking data[23] support the hypothesis that two TRAP molecules are present in each native channel.

Sec61 in the native channel

By analogy with other channels, we suggest that multiple copies of the Sec61 complex may be arranged with local symmetry under the ribosome. Previous studies have shown that the heterotrimeric SecY complex may form a dimer in detergent and in 2D membrane crystals, where the TM segments of the essential SecE subunits face each other.[5,9,10,12] Experimental support for this interaction has been obtained for SecY complexes engaged in translocation.[9,32] A tetramer of SecY was observed by sedimentation equilibrium studies[33] and after solubilizing a membrane complex assembled with SecA.[5] In addition, four density peaks were observed in Sec61 and SecY particles.[3,4] When taken together, these data suggest that two Sec61 dimers may form the channels in our reconstructions.

Archaebacterial SecY and eukaryotic Sec61 complexes each have 12 TM segments and are similar in structure.[9] Thus, we used crystal structures of SecY[9,10] to evaluate the composition and general arrangement of Sec61 in the mammalian channel. To obtain an initial model for two dimers of Sec61, we fit the crystal structure of the archaebacterial SecY complex into the density map from the 2D crystals.[10] We then adjusted the lateral packing of two adjacent dimers in the map from 2D crystals, since there are three extra TMs in the *E. coli* SecY complex, and filtered the resulting model to 20 Å resolution (Figure 6(e)). This subunit arrangement creates a central depression between the four SecY complexes (cd, Figure 6(e)). This feature was interpreted as a translocation pore in previous 3D maps of the channel,[6,34] because it was difficult to assign an accurate threshold when the atomic structure of the ribosome was not known. This central depression may, in fact, contain lipids when the channel is embedded in a membrane. We also note that the lateral packing of a pair of SecY dimers creates a "dimer of dimers" that may lead to an extended ribbon, as occurs in the membrane crystals.[10] Thus, we suggest that connections to the ribosome may introduce perturbations that prevent this lateral polymerization.

We next docked a pair of dimers into the 3D map of the purified Sec61 channel, by aligning the central depression with a similar low density feature in the channel. We also found that the purified Sec61 channel segments into roughly four parts at higher thresholds, and we placed the pair of dimers into the map to maximize the overlap of the subunits with these features (not shown). Since the purified Sec61 channel was accurately docked within the native channel, this fitting process also places the pair of SecY dimers nicely within the native channel (Figure 6(f)). Intriguingly, we find that a pair of dimers can be docked into the channel in two orientations, related by an in-plane rotation of ~90° (only one orientation is shown). This ambiguity arises from the nearly square outline of a pair of dimers (Figure 6(e)), coupled with the modest resolution of our maps. Both models place cytoplasmic features of Sec61 implicated in ribosome binding[9,35] close to the observed connections. Hence, this criterion cannot be used to choose between the models.

While we are not able to choose between these two general models, the analysis clearly favors the hypothesis that four Sec61 complexes are present in purified and native channels. The modeling also supports the idea that Sec61 may associate under the ribosome as a pair of dimers, rather than as a tetramer with *C*4 symmetry. Indeed, our analysis shows that models with Sec61 tetramers can be excluded, because they create a large pore at the center of the channel and a strong modulation of its outer surface (Image 2, Supplementary Material). Neither of these features have been observed.[7,8] Remarkably, we find that putative translocation pores located at the centers of two Sec61 subunits must lie behind the picket fence connections (red circles) in both models. As an example, the model in Figure 6(e) is shown in Figure 6(f). Hence, cryptic pores at the back of the channel may not be accessible to a nascent chain emerging from the tunnel exit (white dot in Figure 6(f)).

Discussion

The present work provides 3D maps of the RCC that show new features of the junction and the protein translocation channel. We also identified TRAP as a ubiquitous component of the mammalian translocon. We suggest that the translocation channel may be created by the lateral association of two Sec61 dimers and in higher eukaryotes, the channel may contain two molecules of TRAP. When taken together, these results have implications for our understanding of protein translocation.

The TRAP complex

Previous experiments showed that TRAP, like Sec61, is an abundant ER protein that stably associates with membrane-bound ribosomes after solubilization.[6,36,37] Our studies show that TRAP is present in every native channel, where it maintains a precise orientation relative to Sec61 and the ribosome. This conclusion is based on experiments in which TRAP was depleted and added-back to RCCs. Although these data suggest that TRAP is the additional component in our maps derived from native membranes, in principle TRAP may allow the OST complex to be visualized, even if TRAP itself becomes disordered. We find this explanation unlikely for four reasons. First, the number of TMs in OST (~27) cannot be accommodated in our map

of the native channel, after accounting for four Sec61 complexes. Second, the predicted size of the OST lumenal domain is much too large to account for the lumenal domain in our map. Third, we found that OST can bind to RCCs in the absence of TRAP, which would preclude this scenario. Fourth, we have obtained a 3D map of canine OST (J.M. *et al.*, unpublished results) and features of this complex are distinct from those in the native channel map. Thus, while OST is present in our specimen prepared from native membranes, we conclude that it may become disordered during isolation or on the EM grid.

TRAP forms three structural domains in the channel: a membrane-embedded region with extensive interactions to Sec61, a primary stalk and a lumenal domain with an additional stalk-like connection (Figure 7(a) and (b)). Sequence conservation of TRAPα and β subunits and the size of their predicted lumenal segments, suggests that these subunits form a major part of the lumenal domain. In addition, the size of the membrane-embedded region, after subtracting the contribution of Sec61, indicates that the native channel may contain two TRAP complexes. This hypothesis is supported by crosslinking studies of TRAP in membranes[23] and by the mobility of purified TRAP on sucrose gradients (R.S.H., unpublished results). In our model, two TRAP molecules interact with a pair of Sec61 dimers and also associate to form a single lumenal domain (Figure 7(b)). This general organization is reminiscent of the structure of an L-type calcium channel, which is comprised of a tetramer of α-subunits with a finger-like domain that emanates from only one side.[38]

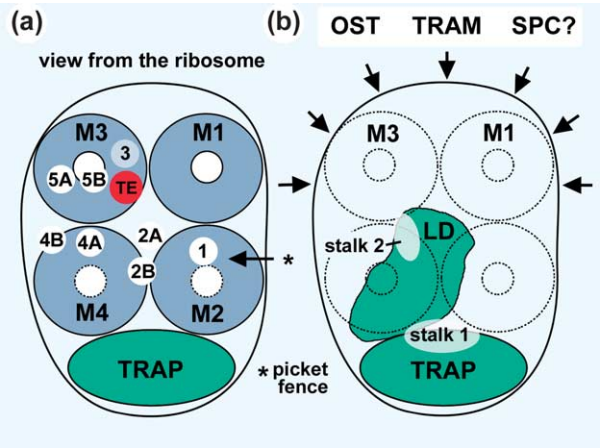

Figure 7. General architecture of the native, protein translocation channel. (a) A diagram of the ribosome channel complex is shown, as viewed from the ribosome. The native channel is formed by four Sec61 complexes (blue circles) and two copies of the TRAP complex (green ellipse). The precise orientation of the unique Sec61 dimers is not known. However, individual pores (white circles) have similar positions for both models. The relative positions of the connections, the picket fence and the tunnel exit (red circle, TE) are shown. Putative translocation pores in monomers M2 and M4 lie behind the picket fence in both models and thus, may be inactive. Connection 3 is rather weak in the current maps. (b) The positions of the TRAP lumenal domain (LD), stalks (white ellipses marked 1 and 2) and the trans-membrane domain (green ellipse) are shown, relative to the channel. The primary stalk and lumenal domain is formed by TRAP α and β-subunits, but the δ-subunit may also contribute. The position of TRAP, coupled with its size, suggests that OST, TRAM and the SPC may approach the front of the channel (black arrows), to interact with the nascent chain.

In previous studies, TRAP was shown to improve the translocation efficiency of some substrates, but not others.[21] In addition, the TRAP α-subunit can be crosslinked to preprolactin chains on the lumenal side of the ER membrane.[17] Our studies indicate that TRAP is present in most ribosome-bound channels in the canine ER.[31] Thus, we suggest that it may have a general role in protein translocation in higher eukaryotes. Indeed, the lumenal domain is ideally positioned to interact with a nascent polypeptide chain emerging from Sec61 (Figure 7(b)) or alternatively, TRAP may recruit a lumenal ER protein to interact with the incoming polypeptide.

The role of Sec61 in protein translocation

Our models show that the protein translocation channel is comprised of four Sec61 complexes, but there are two possibilities for their arrangement in the channel as a pair of dimers. In model 1, a Sec61 dimer may be formed by monomers M1 and M2 (also M3/M4; Figure 7(a)), while in model 2 a dimer may be formed by monomers M1 and M3 (also M2/M4). This ambiguity is due to the modest resolution of our current maps of the channel (~20 Å), coupled with the roughly square shape of a pair of Sec61 dimers. While the proposed side-by-side packing of dimers is unusual, certain features are reminiscent of ionotrophic glutamate receptors in which four subunits associate as a dimer of dimers, rather than as a tetramer.[39]

The four copies of Sec61 in the channel make different connections with the ribosome, due to its asymmetric structure. Thus, monomers M2, M3 and M4 may make multiple connections to the large subunit, while M1 appears to have no direct connection. The ribosome–channel junction is also more crowded than seen previously,[7,8] but may still allow cytosolic domains of membrane proteins to move through the gap and into the cytosol. This gap may also contain flexible segments of ribosomal proteins and Sec61 subunits, but these segments may not provide a serious obstacle to movements of a nascent chain. In addition, the connections themselves may be somewhat flexible, as suggested by the observed difference in resolution between the two partners in our maps.

Our results support the idea that the translocation pore may not be located centrally at the interface between Sec61 complexes. Thus, we find that there is a central depression in the assembly (also see the work done by Beckmann *et al.*[7] and Morgan *et al.*[8]), rather than a large aqueous pore.[6,34] Our data are

also consistent with the crystal structure of SecY, which indicates that lateral surfaces of the channel subunit are inappropriate to create a large, hydrophilic pore, because these surfaces are hydrophobic.[9,11] We suggest that the depression located at the confluence of four Sec61 complexes may be filled with lipid when the channel is embedded in a membrane and it may be partly occupied by detergent in our specimens.

The crystal structure of SecY suggests that the pore may be formed by a single copy of the Sec61 complex;[9] hence there are four possible pores in the channel, one for each subunit. However, our results place constraints on the roles of Sec61 in the channel. Regardless of the precise arrangement of Sec61 subunits in the channel, two copies (M2 and M4) would be separated from the tunnel exit site by a line of connections (Figure 7(a)), making them inaccessible to the nascent chain. While it is premature to decide which of the remaining subunits at the front of the channel may be active, we note that the pore in one subunit may be partially blocked by connections 5A and 5B (Figure 7(a)). Thus, the pore in monomer 1 may be more readily accessible to a nascent chain as it emerges from the tunnel exit. In addition, the distance from the peptidyl transferase center to both possible pores at the front of the channel is consistent with the observation that ~63–68 residues of a nascent chain are protected from proteolysis.[40] Thus, additional studies are now needed to identify the active subunit.

If a single Sec61 can translocate a nascent chain, as suggested by the crystal structure of SecY,[9] then what is the role of the other copies of Sec61 in the channel? First, the association of TRAP with Sec61 at the back of the channel suggests that two copies of Sec61 may recruit TRAP to the translocation site, while also forming connections to the ribosome. Other factors such as signal peptidase, the oligosaccharide transferase and TRAM may also be recruited to the translocation site by lateral interactions with Sec61 (Figure 7(b)). Second, oligomerization of Sec61 may be required to make the ribosome–channel junction more stable, since a single Sec61 complex may not be sufficient to create an open junction while also forming a conduit for the nascent chain. Third, channel assembly and formation of the picket fence connections may help displace SRP and (possibly SR) from the ribosome, due to overlapping binding sites on the large subunit.[41,42] Finally, oligomer formation by Sec61 may set the stage so that the active subunit in the channel makes minimal contact with the ribosome, which would allow this subunit to undergo conformational changes during translocation.

Materials and Methods

Preparation of ribosome–channel complexes

A total extract of canine ER membranes was prepared using DBC (pH 7.5).[21] TRAP was depleted from canine ER extracts using Q-Sepharose under high salt conditions, as described.[16,21] Purification of porcine TRAP, replenishment of canine ER detergent extracts, proteoliposome reconstitution, immuno-blots and translocation assays were carried out as described.[21] Native RCCs were made by adding canine ribosomes with an E-site tRNA to ribosome-stripped proteoliposomes.[8] The complexes were then floated, solubilized, concentrated and prepared for electron cryo-microscopy as described.[8] In some cases, carbon-coated EM grids were briefly wetted with poly-lysine (180 residues at 0.01 mg/ml). These grids were then rinsed in buffer before RCCs were added, blotted at 4 °C in a humid chamber and plunged into liquid ethane to vitrify the samples.

Electron cryo-microscopy and image processing

Frozen grids were mounted on a Gatan cryo-holder (626-DH) and images recorded on a Tecnai F20 at 50,000X (for native RCCs) or at 29,000X (for TRAP-depleted and TRAP add-back specimens). Micrographs were recorded on Kodak SO163 film and developed for 12 minutes. Images that exhibited astigmatism, drift or defocus gradients were eliminated. The micrographs were scanned with a 4.5 μm raster on an Eversmart Supreme scanner (Creo Inc.). The 8-bit data were binned 3×3 (for native RCCs/pixel size=2.73 Å) and 2×2 (for the Trap-depleted and add-back specimens/pixel size=3.14 Å) and converted to SPIDER[43] and EMAN[25] compatible formats. Particles were windowed with BOXER in EMAN using projections of a 3D model. CTF parameters were determined by interactive fitting of summed power spectra with CTFIT and the images were subsequently CTF corrected by phase flipping particles in the TRAP-depleted and add-back datasets. Datasets for the two native RCC maps were corrected in EMAN by phase flipping and by using an experimentally measured structure factor for the ribosome to model the amplitude fall-off.

Native RCC datasets prepared without and with TRAP were computationally purified with the *multirefine* option in EMAN,[44] using 3D volumes that contained the ribosome and the appropriate RCC as references.[6,8] These particle images were refined in separate groups using Radon methods implemented in SPIDER to produce the final 3D volumes.[8,45] Datasets for native RCCs were aligned in EMAN on a 32 processor Linux cluster. The resolution in all cases was ascertained using the FSC 0.5 criteria. Resolution curves for the ribosome and channel were determined with half-datasets from even and odd particles, after separating the maps into sub-volumes using QSegment in EMAN. We choose surface thresholds based on the fit between the atomic structures of the docked ribosomal subunits and the corresponding regions in the maps. At this threshold, the channel is well connected to the large subunit. The final 3D volumes were segmented in EMAN to give separate maps of the small and large subunit, as well as the channel. Figures were made in WEB,[42] O,[46] GIMP† and Adobe Photoshop.

† www.gimp.org

Acknowledgements

We thank A. Neuhof for help in preparing native RCCs, D. Centrella for scanning and particle selection and W. Clemons Jr and E. Hartmann for helpful discussions. T.A.R. is an investigator of the Howard Hughes Medical Institute. Work in the T.A.R. and C.W.A. laboratories was supported by NIH grants.

Supplementary Data

Supplementary data associated with this article can be found, in the online version, at doi:10.1016/j.jmb.2005.02.053

References

1. Rapoport, T. A., Jungnickel, B. & Kutay, U. (1996). Protein transport across the eukaryotic endoplasmic reticulumn and bacterial inner membranes. *Annu. Rev. Biochem.* **65**, 271–303.
2. Johnson, A. E. & Waes, M. A. (1999). The translocon: a dynamic gateway at the ER membrane. *Annu. Rev. Cell Dev. Biol.* **15**, 799–842.
3. Hanein, D., Matlack, K. E. S., Jungnickel, B., Plath, K., Kalies, K.-U., Miller, K. R. *et al*. (1996). Oligomeric rings of the Sec61p complex induced by ligands required for protein translocation. *Cell*, **87**, 721–732.
4. Meyer, T. H., Ménétret, J. F., Breitling, R., Miller, K. R., Akey, C. W. & Rapoport, T. A. (1999). The bacterial SecY/E translocation complex forms channel-like structures similar to those of the eukaryotic Sec61p complex. *J. Mol. Biol.* **285**, 1789–1800.
5. Manting, E. H., van Der Does, C., Remigy, H., Engel, A. & Driessen, A. J. (2000). SecYEG assembles into a tetramer to form the active protein translocation channel. *EMBO J.* **19**, 852–861.
6. Ménétret, J. F., Neuhof, A., Morgan, D. G., Plath, K., Radermacher, M., Rapoport, T. A. & Akey, C. W. (2000). The structure of ribosome–channel complexes engaged in protein translocation. *Mol. Cell.* **6**, 1219–1232.
7. Beckmann, R., Spahn, C. M., Eswar, N., Helmers, J., Penczek, P. A., Sali, A. *et al*. (2001). Architecture of the protein-conducting channel associated with the translating 80 S ribosome. *Cell*, **107**, 361–372.
8. Morgan, D. G., Ménétret, J. F., Neuhof, A., Rapoport, T. A. & Akey, C. W. (2002). Structure of the mammalian ribosome–channel complex at 17 Å resolution. *J. Mol. Biol.* **324**, 871–886.
9. van den Berg, B., Clemons, W. M., Jr, Collinson, I., Modis, Y., Hartmann, E., Harrison, S. C. & Rapoport, T. A. (2004). X-ray structure of a protein-conducting channel. *Nature*, **427**, 36–44.
10. Breyton, C., Haase, W., Rapoport, T. A., Kuhlbrandt, W. & Collinson, I. (2002). Three-dimensional structure of SecYEG, the bacterial protein–translocation complex. *Nature*, **418**, 662–664.
11. Clemons, W. M., Jr, Ménétret, J. F., Akey, C. W. & Rapoport, T. A. (2004). Structural insight into the protein translocation channel. *Curr. Opin. Struct. Biol.* **14**, 390–396.
12. Bessonneau, P., Besson, V., Collinson, I. & Duong, F. (2002). The SecYEG preprotein translocation channel is a conformationally dynamic and dimeric structure. *EMBO J.* **21**, 995–1003.
13. Matlack, K. E. S., Mothes, W. & Rapoport, T. A. (1998). Protein translocation-tunnel vision. *Cell*, **92**, 381–390.
14. Martoglio, B., Hofmann, M. W., Brunner, J. & Dobberstein, B. (1995). The protein-conducting channel in the membrane of the endoplasmic reticulum is open laterally toward the lipid bilayer. *Cell*, **81**, 207–214.
15. Knauer, R. & Lehle, L. (1999). The oligosaccharyltransferase complex from yeast. *Biochim. Biophys. Acta*, **1426**, 259–273.
16. Görlich, D. & Rapoport, T. A. (1993). Protein translocation into proteoliposomes reconstituted from purified components of the endoplasmic reticulum membrane. *Cell*, **75**, 615–630.
17. Mothes, W., Prehn, S. & Rapoport, T. A. (1994). Systematic probing of the environment of a translocating secretory protein during translocation through the ER membrane. *EMBO J.* **13**, 3973–3982.
18. Do, H., Falcone, D., Lin, J., Andrews, D. W. & Johnson, A. E. (1996). The cotranslational integration of membrane proteins into the phospholipid bilayer is a multistep process. *Cell*, **85**, 369–378.
19. Voigt, S., Jungnickel, B., Hartmann, E. & Rapoport, T. A. (1996). Signal-sequence dependent function of the TRAM protein during early phases of protein transport across the ER membrane. *J. Cell Biol.* **134**, 25–35.
20. Hartmann, E., Görlich, D., Kostka, S., Otto, A., Kraft, R., Knespel, S. *et al*. (1993). A tetrameric complex of membrane proteins in the endoplasmic reticulum. *Eur. J. Biochem.* **214**, 375–381.
21. Fons, R. D., Bogert, B. A. & Hegde, R. S. (2003). The translocon-associated protein complex facilitates the initiation of substrate translocation across the ER membrane. *J. Cell Biol.* **160**, 529–539.
22. Wiedmann, M., Görlich, D., Hartmann, E., Kurzchalia, T. V. & Rapoport, T. A. (1989). Photocrosslinking demonstrates proximity of a 34 kDa membrane protein to different portions of preprolactin during translocation through the endoplasmic reticulum. *FEBS Letters*, **257**, 263–268.
23. Görlich, D., Prehn, S., Hartmann, E., Herz, J., Otto, A., Kraft, R. *et al*. (1990). The signal sequence receptor has a second subunit and is part of a translocation complex in the endoplasmic reticulum as probed by bifunctional reagents. *J. Cell Biol.* **111**, 2283–2294.
24. Görlich, D., Hartmann, E., Prehn, S. & Rapoport, T. A. (1992). A protein of the endoplasmic reticulum involved early in polypeptide translocation. *Nature*, **357**, 47–52.
25. Ludtke, S. J., Baldwin, P. R. & Chiu, W. (1999). EMAN: semiautomated software for high-resolution single-particle reconstructions. *J. Struct. Biol.* **128**, 82–97.
26. Gerbi, S. A. (1996). Expansion segments: regions of variable size that interrupt the universal core secondary structure of ribosomal RNA. In *Ribosomal RNA, Structure, Evolution, Processing, and Function in Protein Biosynthesis* (Zimmermann, R. A. & Dahlberg, A. E., eds), pp. 71–87, CRC Press, New York.
27. Dube, P., Bacher, G., Stark, H., Mueller, F., Zemlin, F., van Heel, M. & Brimacombe, R. (1998). Correlation of the expansion segments in mammalian rRNA with the fine structure of the 80 S ribosome: a cryo-electron microscopic reconstruction of the rabbit reticulocyte ribosome at 21 Å resolution. *J. Mol. Biol.* **279**, 403–421.
28. Morgan, D. G., Ménétret, J. F., Rademacher, M.,

Neuhof, A., Akey, I. V., Rapoport, T. A. & Akey, C. W. (2000). A comparison of the yeast and the rabbit 80 S ribosome reveals the topology of the nascent chain exit tunnel, inter-subunit bridges and mammalian rRNA expansion segments. *J. Mol. Biol.* **301**, 301–321.
29. Wimberly, B., Brodersen, D. E., Clemons, W. M., Jr, Morgan-Warren, R. J., Carter, A. P., von Rhein, C. *et al*. (2000). Structure of the 30 S ribosomal subunit. *Nature*, **407**, 327–339.
30. Ban, N., Nissen, P., Hansen, J., Moore, P. B. & Steitz, T. A. (2000). The complete atomic structure of the large ribosomal subunit at 2.4 Å resolution. *Science*, **289**, 905–920.
31. Snapp, E. L., Reinhart, G. A., Bogert, B. A., Lippincott-Schwartz, J. & Hegde, R. S. (2004). The organization of engaged and quiescent translocons in the endoplasmic reticulum of mammalian cells. *J. Cell Biol.* **164**, 997–1007.
32. Kaufmann, A., Manting, E. H., Veenendaal, A. K., Driessen, A. J. & van der Does, C. (1999). Cysteine-directed cross-linking demonstrates that helix 3 of SecE is close to helix 2 of SecY and helix 3 of a neighboring SecE. *Biochemistry*, **38**, 9115–9125.
33. Collinson, I., Breyton, C., Duong, F., Tziatzios, C., Schubert, D., Or, E. *et al*. (2001). Projection structure and oligomeric properties of a bacterial core protein translocase. *EMBO J.* **20**, 2462–2471.
34. Beckmann, R., Bubeck, D., Grassucci, R., Penczek, P., Verschoor, A., Blobel, G. & Frank, J. (1997). Alignment of conduits for the nascent polypeptide chain in the ribosome–Sec61 complex. *Science*, **19**, 2123–2126.
35. Raden, D., Song, W. & Gilmore, R. (2000). Role of the cytoplasmic segments of Sec61alpha in the ribosome-binding and translocation-promoting activities of the Sec61p complex. *J. Cell Biol.* **150**, 53–64.
36. Hartmann, E., Wiedmann, M. & Rapoport, T. A. (1989). A membrane component of the endoplasmic reticulum that may be essential for protein translocation. *EMBO J.* **8**, 2225–2229.
37. Görlich, D., Prehn, S., Hartmann, E., Kalies, K. U. & Rapoport, T. A. (1992). A mammalian homolog of Sec61p and SecYp is associated with ribosomes and nascent polypeptides during translocation. *Cell*, **71**, 489–503.
38. Wolf, M., Eberhart, A., Glossmann, H., Striessnig, J. & Grigorieff, N. (2003). Visualization of the domain structure of an L-type Ca2+ channel using electron cryo-microscopy. *J. Mol. Biol.* **332**, 171–182.
39. Tichelaar, W., Safferling, M., Keinanen, K., Stark, H. & Madden, D. R. (2004). The three-dimensional structure of an ionotropic glutamate receptor reveals a dimer-of-dimers assembly. *J. Mol. Biol.* **344**, 435–442.
40. Jungnickel, B. & Rapoport, T. A. (1995). A posttargeting signal-sequence recognition event in the endoplasmic reticulum membrane. *Cell*, **82**, 261–270.
41. Halic, M., Becker, T., Pool, M. R., Spahn, C. M., Grassucci, R. A., Frank, J. & Beckmann, R. (2004). Structure of the signal recognition particle interacting with the elongation-arrested ribosome. *Nature*, **427**, 808–814.
42. Mandon, E. C., Jiang, Y. & Gilmore, R. (2003). Dual recognition of the ribosome and the signal recognition particle by the SRP receptor during protein targeting to the endoplasmic reticulum. *J. Cell Biol.* **162**, 575–585.
43. Frank, J., Radermacher, M., Penczek, P., Zhu, J., Li, Y., Ladjadj, M. & Leith, A. (1996). SPIDER and WEB: processing and visualization of images in 3D electron microscopy and related fields. *J. Struct. Biol.* **116**, 190–199.
44. Brink, J., Ludtke, S. J., Kong, Y., Wakil, S. J., Ma, J. & Chiu, W. (2004). Experimental verification of conformational variation of human fatty acid synthase as predicted by normal mode analysis. *Structure*, **12**, 185–191.
45. Radermacher, M. (1994). Three-dimensional reconstitution from Radon projections: orientational alignment *via* Radon transforms. *Ultramicroscopy*, **53**, 121–136.
46. Jones, T. A., Zou, J.-Y., Cowan, S. W. & Kjeldgaard, M. (1991). Improved methods for building protein models in electron density maps and the location of errors in these models. *Acta Crystallog. sect. A*, **47**, 110–119.

Edited by W. Baumeister

(Received 6 December 2004; received in revised form 13 February 2005; accepted 21 February 2005)